

# An Equivalent Model for Wiring Harness Induced Current in Automobiles

Y. Zheng<sup>1</sup>, Q. Wang<sup>1</sup>, G. Wang<sup>2</sup>, Z. An<sup>1</sup>, Q. Liu<sup>1</sup>, and X. Li<sup>3</sup>

<sup>1</sup> State Key Laboratory of Power Transmission Equipment & System Security and New Technology, Chongqing University, Chongqing 400040, China  
yaya9304@163.com, wangquandi@cqu.edu.cn, anzongyu123@163.com, lqs234@163.com

<sup>2</sup> Chengdu Qingbaijiang Power Supply Company of the State Grid, Chengdu 610300, China  
cqu2002wgh@163.com

<sup>3</sup> Changan Automotive Engineering Institute, Chongqing 401120, China  
lixu@changan.com.cn

**Abstract** – This paper presents an equivalent model for the simulation of the induced current along wiring harnesses in automobiles. The equivalent model is based on multi-transmission line theory. Then, this model is simulated by using the commercial FEM software, HFSS. The common-mode current simulation results show that the presented method is effective and the equivalent model can reduce the computation time and complexity of the wire harness model. Finally, the proposed equivalent method is proved by experiment. The equivalent model can handle automotive wiring harness for electromagnetic radiation sensitivity problems in the high frequency range.

**Index Terms** – Electromagnetic radiation sensitivity, electromagnetic compatibility, equivalent model, multi-conductor transmission line, induced current, and wiring harness.

## I. INTRODUCTION

With increasing electronic devices in automobiles, electromagnetic compatibility (EMC) becomes extremely important. To improve the design and the production of the automobiles, the full numerical model of a car has become a strategic challenge in automotive industries [1, 2]. The automobile EMC models include car body, wiring harnesses and electrical component models,

which indicate the importance of wiring harness modeling [3].

Several studies on the electromagnetic radiation sensitivity of conductors have been performed by using the methods of Taylor, Agrawal, and Rachidi [4-7], as well as the extension of these methods [8-11]. These methods are based on multi-conductor transmission line (MTL) theory. The voltage source or current source, instead of the incident wave, is placed in an equivalent lumped-circuit model to calculate the terminal response. Numerous automotive wiring harnesses cannot always satisfy the approximate conditions of the above mentioned methods, such as the distance between the conductors must be larger than the wire radius and smaller than the incident wave length. The complex wiring harnesses are handled as a single conductor in [12] and this simple model ignores the electromagnetic characteristic differences due to terminal loads. The Agrawal model was developed according to electromagnetic topology theory, which dealt with the wiring harnesses one by one while establishing the model [13]. However, this modeling process becomes very complex when harnesses are too many. A method simplified cable bundles in [14], which is according to its characteristic impedance and used the method of moments (MoM) to obtain the common-mode current inducted on the conductors by the incident wave. This simplified method

decreases the complexity of modeling. However, the definition of the common-mode characteristic impedance of harness was not presented.

The present paper proposes a method to simplify the wiring harness model. First, the definition of wiring harness equivalent wave impedance is shown and the calculation formula is deduced to clarify the computing method. The wiring harness group method is then described in detail. The induced current generated by the incident wave can be calculated based on the FEM, which is detailed in the paper. The equivalent model is demonstrated by a numerical example and an experiment. The terminal load equivalent method is also verified.

## II. THE EQUIVALENT MODEL

### A. Equivalence principle

#### 1) Equivalent wave impedance

Figure 1 shows the multi-conductors transmission line system.  $r_p$  and  $r_q$  are the radii of the conductors  $p$  and  $q$ , respectively;  $h_p$  and  $h_q$  are the heights of the conductors  $p$  and  $q$  above the ground reference, respectively;  $s_{pq}$  is the distance between conductors  $p$  and  $q$ ;  $s_{pq'}$  is the distance between conductor  $p$  and mirror conductor  $q'$ .

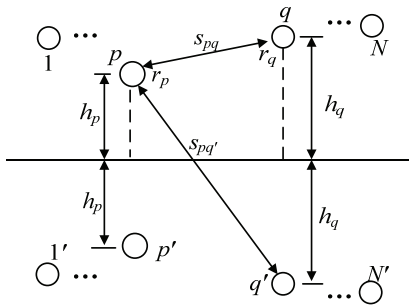


Fig. 1. Multi-conductor transmission line system.

If the electric charge of each per-unit-length (p.u.l) conductor is  $Q_1, Q_2, \dots, Q_N$ , then each conductor voltage to ground reference ( $V_1, V_2, \dots, V_N$ ) can be written as [15],

$$\begin{cases} V_1 = \eta_{11}Q_1 + \eta_{12}Q_2 + \dots + \eta_{1N}Q_N \\ V_2 = \eta_{21}Q_1 + \eta_{22}Q_2 + \dots + \eta_{2N}Q_N \\ \dots \\ V_N = \eta_{N1}Q_1 + \eta_{N2}Q_2 + \dots + \eta_{NN}Q_N \end{cases} \quad (1)$$

where  $\eta$  is potential coefficient, which can be calculated as follows,

$$\begin{cases} \eta_{pp} = \frac{1}{2\pi\epsilon_0} \ln \frac{2h_p}{r_p} \\ \eta_{pq} = \frac{1}{2\pi\epsilon_0} \ln \frac{s_{pq'}}{s_{pq}} = \frac{1}{4\pi\epsilon_0} \ln \left( 1 + \frac{4h_p h_q}{s_{pq}^2} \right) \end{cases} \quad (2)$$

where  $\epsilon_0$  is the dielectric coefficient of air,  $\eta_{pq} = \eta_{qp}$ ,  $p, q = 1, 2, \dots, N, p \neq q$ .

When the right side is multiplied by  $v/v$  ( $v = 1/\sqrt{\mu_0 \epsilon_0}$ ), equation (1) can be rewritten as follows,

$$\begin{cases} V_1 = \xi_{11}I_1 + \xi_{12}I_2 + \dots + \xi_{1N}I_N \\ V_2 = \xi_{21}I_1 + \xi_{22}I_2 + \dots + \xi_{2N}I_N \\ \dots \\ V_N = \xi_{N1}I_1 + \xi_{N2}I_2 + \dots + \xi_{NN}I_N \end{cases} \quad (3)$$

where  $\xi$  is the conductor wave impedance and can be easily obtained,

$$\begin{cases} \xi_{pp} = \frac{\eta_{pp}}{v} = \frac{1}{2\pi} \sqrt{\frac{\mu_0}{\epsilon_0}} \ln \frac{2h_p}{r_p} \\ \xi_{pq} = \frac{\eta_{pq}}{v} = \frac{1}{4\pi} \sqrt{\frac{\mu_0}{\epsilon_0}} \ln \left( 1 + \frac{4h_p h_q}{s_{pq}^2} \right) \end{cases} \quad (4)$$

We define the wiring harness equivalent wave impedance as the ratio of the voltage and the sum of the currents on all conductors in the case of the same voltage,

$$\xi_{eq} = \frac{V}{I_1 + I_2 + \dots + I_N} = \frac{1}{\sum_{p=1}^N \sum_{q=1}^N A_{pq} / |\xi|} \quad (5)$$

where  $A_{pq}$  is the algebraic of the element  $\xi_{pq}$ , and  $|\xi|$  is the determinant of the matrix  $[\xi]$ . The wiring harness equivalent wave impedance contains self- and mutual-wave impedance and depends on the structure of the conductors.

#### 2) Grouping method

The terminal grounded load and equivalent wave impedance determine the electromagnetic characteristics of the transmission line [1]. Thus, the conductors can be grouped as shown in Table I. In Table I,  $|Z_{pj}|$  and  $j$  ( $j=1, 2$ ) are the terminal grounded load and the terminal number of the conductor  $p$ , respectively. If the terminal ground load is the same as the equivalent wave impedance, the conductor achieves matching condition and can be grouped flexibly. For example, if  $|Z_{p1}| < \xi_{eq}$  and  $|Z_{p2}| = \xi_{eq}$ , the conductor can be classified under the first or the second equivalent group. The conductors are physically adjacent to each other in the same group, otherwise, the error of simulation results will increase.

Table I: Conductor classification table.

	End 1 ( $j=1$ )	End 2 ( $j=2$ )
First equivalent conductor group (G1)	$ Z_{p1}  < \zeta_{eq}$	$ Z_{p2}  < \zeta_{eq}$
Second equivalent conductor group (G2)	$ Z_{p1}  < \zeta_{eq}$	$ Z_{p2}  > \zeta_{eq}$
Third equivalent conductor group (G3)	$ Z_{p1}  > \zeta_{eq}$	$ Z_{p2}  < \zeta_{eq}$
Fourth equivalent conductor group (G4)	$ Z_{p1}  > \zeta_{eq}$	$ Z_{p2}  > \zeta_{eq}$

## B. Equivalent model

### 1) P.u.l. capacitance and inductance matrix

By neglecting the resistance and conductance, the transmission line equations become only relevant to the capacitance and inductance [16],

$$\frac{\partial}{\partial z} \begin{bmatrix} I_1 \\ I_2 \\ \vdots \\ I_N \end{bmatrix} = -j\omega \begin{bmatrix} C_{11} & C_{12} & \cdots & C_{1N} \\ C_{21} & C_{22} & \cdots & C_{2N} \\ \vdots & \vdots & \ddots & \vdots \\ C_{N1} & C_{N2} & \cdots & C_{NN} \end{bmatrix} \begin{bmatrix} V_1 \\ V_2 \\ \vdots \\ V_N \end{bmatrix} \quad (6)$$

$$\frac{\partial}{\partial z} \begin{bmatrix} V_1 \\ V_2 \\ \vdots \\ V_N \end{bmatrix} = -j\omega \begin{bmatrix} L_{11} & L_{12} & \cdots & L_{1N} \\ L_{21} & L_{22} & \cdots & L_{2N} \\ \vdots & \vdots & \ddots & \vdots \\ L_{N1} & L_{N2} & \cdots & L_{NN} \end{bmatrix} \begin{bmatrix} I_1 \\ I_2 \\ \vdots \\ I_N \end{bmatrix} \quad (7)$$

The p.u.l. capacitance matrix is calculated using FEM since the condition  $d > 5r$  ( $d$  is the distance between conductors and  $r$  is the conductor radius) is not always satisfied in automotive wiring harnesses [17]. The p.u.l. inductance matrix can be obtained using the analysis method [16]. To obtain the p.u.l. capacitance and inductance matrix of the equivalent groups, three hypotheses are made:

(1) The equivalent group current is equal to the sum of the currents induced on all original conductors in the group. The current flowing along the conductor is equal to the average of the equivalent group current. For example, an equivalent group  $m$  contains  $K$  conductors, then the group current  $I_{Gm}$  and the conductor current  $I_k$  ( $k=1, 2, \dots, K$ ) can be written as,

$$\begin{cases} I_{Gm} = I_1 + I_2 + \cdots + I_K \\ I_k = \frac{I_{Gm}}{K} \end{cases} \quad (8)$$

(2) All conductors of the equivalent group have the same electrical potential as compared with the ground reference. Therefore, the group voltage  $V_{Gm}$  equals the conductor voltage, which can be written as,

$$V_{Gm} = V_1 = V_2 = \cdots = V_K \quad (9)$$

(3) Compared with the common-mode currents, the differential-mode currents induced by

electromagnetic wave are negligible.

$N$  conductors are assumed present in the wiring harness and can be classified into four groups, as shown in Table I. The equivalent group 1 contains  $N_1$  conductors of  $1 \sim \alpha$ , the equivalent group 2 contains  $N_2$  conductors of  $\alpha+1 \sim \beta$ , the equivalent group 3 contains  $N_3$  conductors of  $\beta+1 \sim \gamma$ , and the equivalent group 4 contains  $N_4$  conductors of  $\gamma+1$  to  $N$ . Considering the hypotheses, equations (6) and (7) can be simplified as follows,

$$\frac{\partial}{\partial z} \begin{bmatrix} I_{G1} \\ I_{G2} \\ I_{G3} \\ I_{G4} \end{bmatrix} = -j\omega [C]_{eq} \begin{bmatrix} V_{G1} \\ V_{G2} \\ V_{G3} \\ V_{G4} \end{bmatrix} \quad (10)$$

$$\frac{\partial}{\partial z} \begin{bmatrix} V_{G1} \\ V_{G2} \\ V_{G3} \\ V_{G4} \end{bmatrix} = -j\omega [L]_{eq} \begin{bmatrix} I_{G1} \\ I_{G2} \\ I_{G3} \\ I_{G4} \end{bmatrix}, \quad (11)$$

where  $[C]_{eq}$  and  $[L]_{eq}$  are the p.u.l. capacitance matrix and inductance matrix of equivalent conductor groups, respectively. They can be written as follows,

$$[C]_{eq} = \begin{bmatrix} \sum_{p=1}^{\alpha} \sum_{q=1}^{\alpha} C_{pq} & \sum_{p=1}^{\alpha} \sum_{q=\alpha+1}^{\beta} C_{pq} & \sum_{p=1}^{\alpha} \sum_{q=\beta+1}^{\gamma} C_{pq} & \sum_{p=1}^{\alpha} \sum_{q=\gamma+1}^N C_{pq} \\ \sum_{p=\alpha+1}^{\beta} \sum_{q=1}^{\alpha} C_{pq} & \sum_{p=\alpha+1}^{\beta} \sum_{q=\alpha+1}^{\beta} C_{pq} & \sum_{p=\alpha+1}^{\beta} \sum_{q=\beta+1}^{\gamma} C_{pq} & \sum_{p=\alpha+1}^{\beta} \sum_{q=\gamma+1}^N C_{pq} \\ \sum_{p=\beta+1}^{\gamma} \sum_{q=1}^{\alpha} C_{pq} & \sum_{p=\beta+1}^{\gamma} \sum_{q=\alpha+1}^{\beta} C_{pq} & \sum_{p=\beta+1}^{\gamma} \sum_{q=\beta+1}^{\gamma} C_{pq} & \sum_{p=\beta+1}^{\gamma} \sum_{q=\gamma+1}^N C_{pq} \\ \sum_{p=\gamma+1}^N \sum_{q=1}^{\alpha} C_{pq} & \sum_{p=\gamma+1}^N \sum_{q=\alpha+1}^{\beta} C_{pq} & \sum_{p=\gamma+1}^N \sum_{q=\beta+1}^{\gamma} C_{pq} & \sum_{p=\gamma+1}^N \sum_{q=\gamma+1}^N C_{pq} \end{bmatrix} \quad (12)$$

$$[L]_{eq} = \begin{bmatrix} \frac{\sum_{p=1}^{\alpha} \sum_{q=1}^{\alpha} L_{pq}}{N_1^2} & \frac{\sum_{p=1}^{\alpha} \sum_{q=\alpha+1}^{\beta} L_{pq}}{N_1 \cdot N_2} & \frac{\sum_{p=1}^{\alpha} \sum_{q=\beta+1}^{\gamma} L_{pq}}{N_1 \cdot N_3} & \frac{\sum_{p=1}^{\alpha} \sum_{q=\gamma+1}^N L_{pq}}{N_1 \cdot N_4} \\ \frac{\sum_{p=\alpha+1}^{\beta} \sum_{q=1}^{\alpha} L_{pq}}{N_1 \cdot N_2} & \frac{\sum_{p=\alpha+1}^{\beta} \sum_{q=\alpha+1}^{\beta} L_{pq}}{N_2^2} & \frac{\sum_{p=\alpha+1}^{\beta} \sum_{q=\beta+1}^{\gamma} L_{pq}}{N_2 \cdot N_3} & \frac{\sum_{p=\alpha+1}^{\beta} \sum_{q=\gamma+1}^N L_{pq}}{N_2 \cdot N_4} \\ \frac{\sum_{p=\beta+1}^{\gamma} \sum_{q=1}^{\alpha} L_{pq}}{N_1 \cdot N_3} & \frac{\sum_{p=\beta+1}^{\gamma} \sum_{q=\alpha+1}^{\beta} L_{pq}}{N_2 \cdot N_3} & \frac{\sum_{p=\beta+1}^{\gamma} \sum_{q=\beta+1}^{\gamma} L_{pq}}{N_3^2} & \frac{\sum_{p=\beta+1}^{\gamma} \sum_{q=\gamma+1}^N L_{pq}}{N_3 \cdot N_4} \\ \frac{\sum_{p=\gamma+1}^N \sum_{q=1}^{\alpha} L_{pq}}{N_1 \cdot N_4} & \frac{\sum_{p=\gamma+1}^N \sum_{q=\alpha+1}^{\beta} L_{pq}}{N_2 \cdot N_4} & \frac{\sum_{p=\gamma+1}^N \sum_{q=\beta+1}^{\gamma} L_{pq}}{N_3 \cdot N_4} & \frac{\sum_{p=\gamma+1}^N \sum_{q=\gamma+1}^N L_{pq}}{N_4^2} \end{bmatrix} \quad (13)$$

### 2) Structural parameters of the equivalent model [12]

(1) Height of equivalent group,

$$h_{Gm} = \frac{h_1 + h_2 + \dots + h_K}{K} \quad (14)$$

where  $h_1, h_2, \dots, h_K$  is the height above the ground of each conductor in group  $m$  and  $h_{Gm}$  is the height of the equivalent conductor group  $m$  above the ground reference.

(2) Radius of the equivalent group,

$$r_{Gm} = \frac{2h_{Gm}}{\exp\left(\frac{2\pi \cdot L_{mm\_eq}}{\mu_0}\right)} \quad (15)$$

where  $r_{Gm}$  is the equivalent radius of the equivalent conductor group  $m$  and  $L_{mm\_eq}$  is the diagonal element of the equivalent inductance matrix  $[L]_{eq}$ .

(3) Distance between the equivalent groups,

$$d_{Gmn} = \sqrt{\frac{4h_{Gm}h_{Gn}}{\exp\left(\frac{4\pi \cdot L_{mn\_eq}}{\mu_0}\right) - 1}} \quad (16)$$

where  $d_{Gmn}$  is the distance between the equivalent conductor groups  $m$  and  $n$ ;  $h_{Gm}$  and  $h_{Gn}$  are the heights above the ground of the equivalent groups  $m$  and  $n$ , respectively.  $L_{mn\_eq}$  is the non-diagonal element of the equivalent inductance matrix  $[L]_{eq}$ .

(4) Structural parameters adjustment,

Errors may be produced during the equivalent process. For example “ $r_{Gm} + r_{Gn} > d_{mn}$ ” may appear, and the structural parameters must be adjusted. The adjustment process is shown in Fig. 2.

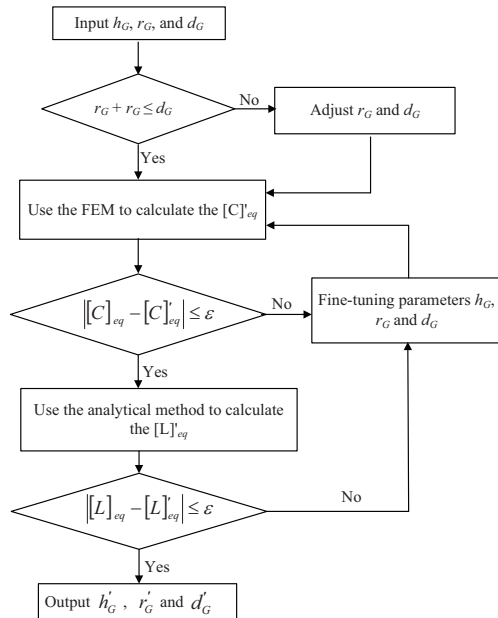


Fig. 2. Flow chart of structural parameters adjustment.

In Fig. 2,  $[C]_{eq}$  is calculated based on the structural parameters from FEM,  $[L]_{eq}$  is calculated based on the structural parameters by analytical method, and  $\varepsilon$  is the computational error. Smaller  $\varepsilon$  corresponds to higher calculation precision. After adjustment, the output structural parameters can establish the equivalent model.

3) Terminal load of the equivalent model [12]

(1) Terminal grounded load,

The terminal grounded load is the load between the conductor and the ground reference. The equivalent grounded load is equal to all the grounded loads in the same equivalent group connected in parallel.

(2) Load between conductors,

If the conductors belong to the same equivalent group, the load between these conductors can be neglected in the equivalent model. However, if the conductors belong to different equivalent groups, load exists between equivalent groups and is equal to the parallel value of all the loads between the conductors.

### III. INDUCED CURRENT

An electric current will be induced in any closed circuit when the magnetic flux through a surface bounded by the conductor changes. Therefore, the induced current can be regarded as an evaluation parameter of the electromagnetic radiation (EMR) sensitivity of the wiring harness.

#### A. Calculation method of the induced current

When a uniform plane wave enters the conductor through the air, the electric and magnetic fields are mutated at the interface for the discontinuousness of the medium, as shown in Fig. 3.

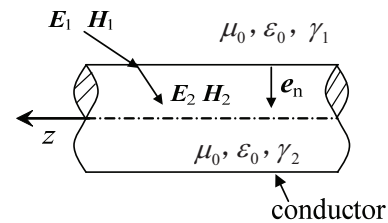


Fig. 3. Uniform plane wave incident on the conductor.

In Fig. 3,  $E_1$  and  $H_1$  are the electric and magnetic field intensities in the air, respectively.

$\mathbf{E}_2$  and  $\mathbf{H}_2$  are the electric and magnetic field intensities in the conductor, respectively.  $\mathbf{e}_n$  is the unit vector normal to the interface pointing from medium 1 to medium 2.

When the electromagnetic wave travels from an ideal medium ( $\gamma_1=0$ ) to an ideal conductor ( $\gamma_2 \rightarrow \infty$ ), the electromagnetic wave will decay to zero quickly. Only a thin layer of the surface current is present on the conductor surface, and the electromagnetic field is almost non-existent in the conductor ( $\mathbf{E}_2 \approx 0$ ,  $\mathbf{H}_2 \approx 0$ ). Using the boundary conditions ( $-\mathbf{e}_n \times \mathbf{H}_1 = \mathbf{K}$ ) and the total fields in the

free space  $\mathbf{H}_1 = \mathbf{e}_k \times \frac{\mathbf{E}_i}{Z_0} - \mathbf{e}_k \times \frac{\mathbf{E}_s}{Z_0}$  ( $Z_0$  is the wave impedance of the air space) [16], the induced current along the conductor is given by equation (17), shown at the bottom of the page. In equation (17),  $\mathbf{e}_{l\perp}$  is the unit vector of the conductor axis, and  $l$  is the closed-loop on the conductor surface.

If the conductor and the reference ground plane are parallel, three coupling modes of the plane wave to the conductor exist, as shown in Fig. 4.

$$\begin{aligned}
 I &= \oint_l (\mathbf{K} \cdot \mathbf{e}_{l\perp}) dl \\
 &= \frac{1}{Z_0} \oint_l [-\mathbf{e}_n \times (\mathbf{e}_k \times \mathbf{E}_i) + \mathbf{e}_n \times (\mathbf{e}_k \times \mathbf{E}_s)] \cdot \mathbf{e}_{l\perp} dl \\
 &= \frac{1}{Z_0} \oint_l \{ [-\mathbf{e}_k (\mathbf{e}_n \cdot \mathbf{E}_i) + \mathbf{E}_i (\mathbf{e}_n \cdot \mathbf{e}_k)] + [\mathbf{e}_k (\mathbf{e}_n \cdot \mathbf{E}_s) - \mathbf{E}_s (\mathbf{e}_n \cdot \mathbf{e}_k)] \} \cdot \mathbf{e}_{l\perp} dl \quad (17) \\
 &= \frac{1}{Z_0} \oint_l \{ (\mathbf{e}_k \cdot \mathbf{e}_{l\perp}) [(\mathbf{e}_n \cdot \mathbf{E}_s) - (\mathbf{e}_n \cdot \mathbf{E}_i)] + (\mathbf{e}_n \cdot \mathbf{e}_k) [(\mathbf{E}_i \cdot \mathbf{e}_{l\perp}) - (\mathbf{E}_s \cdot \mathbf{e}_{l\perp})] \} dl
 \end{aligned}$$

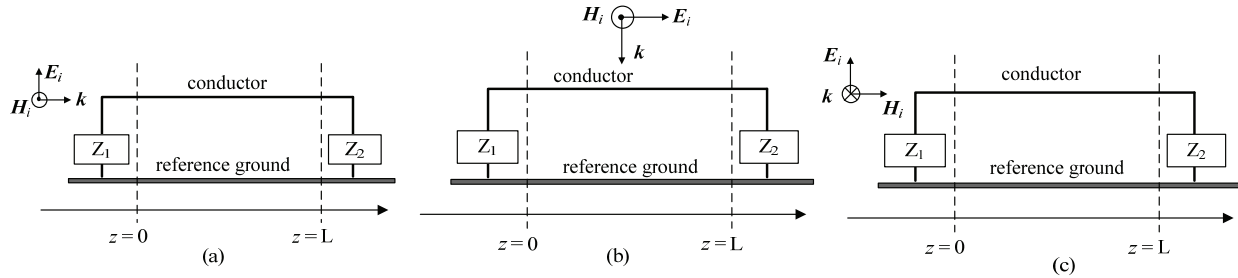


Fig. 4. Three coupling modes of the plane wave to the conductor.

In Fig. 4 (a), the electrical field and the reference ground are orthogonal to each other. The electrical field is named as “vertically polarized wave”. The induced current along the conductor can be obtained using equation (17). Given that  $\mathbf{E}_s = f(\mathbf{E}_i)$ , the induced current along the conductor can be written as,

$$I = \frac{1}{Z_0} \oint_l (\mathbf{e}_k \cdot \mathbf{e}_{l\perp}) [\mathbf{e}_n \cdot (f(\mathbf{E}_i) - \mathbf{E}_i)] dl \quad (18)$$

In Fig. 4 (b), the electrical field and the reference ground are parallel to each other. The electrical field is termed as “horizontally polarized wave”. Therefore, the induced current can be obtained by using equation (17),

$$I = \frac{2}{Z_0} \oint_l (\mathbf{E}_i \cdot \mathbf{e}_{l\perp}) (\mathbf{e}_n \cdot \mathbf{e}_k) dl \quad (19)$$

In Fig. 4 (c),  $\mathbf{e}_k$  and  $\mathbf{E}_s$  are all vertical to  $\mathbf{e}_{l\perp}$ .  $\mathbf{E}_i$  and  $\mathbf{e}_{l\perp}$  are vertical. Based on equation (17), no induced current exists along the conductor.

## B. Effectiveness of the FEM

In the current study, we established a 1 m long uncoated 10-conductor wiring harness model. Figure 5 shows the cross-section geometry. The incident electrical field intensity amplitude is 3 V/m, and the coupling mode is shown in Fig. 6. Table II shows the terminal grounded loads.

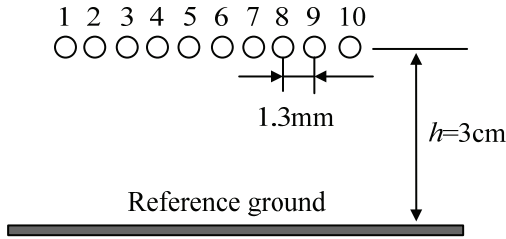


Fig. 5. Cross-section geometry of the wiring harness.

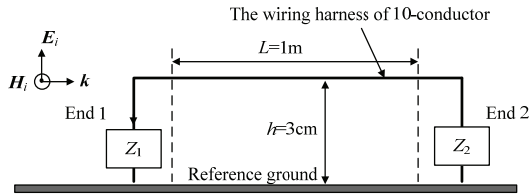


Fig. 6. EMR sensitivity model of the wiring harness.

The induced current calculated at the first end of conductor 4 is simulated based on the FEM and the MTL method, as shown in Fig. 7.

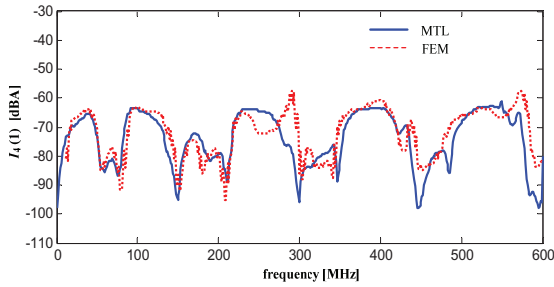


Fig. 7. Current at the first end of conductor 4.

Figure 7 indicates the similarity of the values of the current induced at the first end of the fourth conductor calculated by the FEM and the MTL method. The amplitude differences may have been caused by the differences in the accuracy of the calculation method.

## IV. SIMULATION AND ANALYSIS

### A. Wiring harness and the equivalent model

To validate the proposed method, we used an 80 cm long nine-conductor wiring harness as an example. The distance between the conductors is 2 mm, and the radius is 0.5 mm. The insulating

medium around the conductor is neglected. Table III shows the grounded terminal loads, while Fig. 8 presents the cross-section.

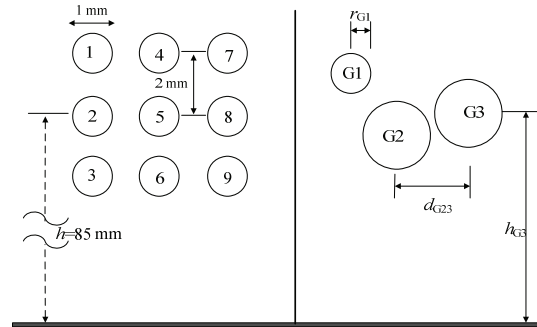


Fig. 8. Cross-section of the original wiring harness (left) and the equivalent model (right).

The wiring harness equivalent wave impedance is  $248.6 \Omega$ . The nine-conductor wiring harness can be divided into three equivalent groups based on the grouping method (indicated in Table I), as shown below:

- 1) Group 1, G1: conductor 1
- 2) Group 2, G2: conductors 2 to 5
- 3) Group 3, G3: conductors 6 to 9.

The nine-conductor p.u.l. capacitance and inductance matrices can be obtained from the structure parameters, as shown in equations (20) and (21) in the next page. The p.u.l. capacitance and inductance matrices of the equivalent group can be obtained using equations (12) and (13),

$$[C]_{\text{eq}} = \begin{bmatrix} 32.5 & -27.9 & -3.2 \\ & 85.4 & -54.7 \\ & & 62.03 \end{bmatrix} \text{ pF/m} \quad (22)$$

$$[L]_{\text{eq}} = \begin{bmatrix} 11704 & 8389 & 7232 \\ & 9204 & 791.4 \\ & & 9105 \end{bmatrix} \text{ nH/m} \quad (23)$$

After applying the four-phase procedure described in section II-B-2, an equivalent model is obtained, which is composed of three equivalent groups:

$r_{G1} = 0.5 \text{ mm}$ ,  $r_{G2} = r_{G3} = 1.5 \text{ mm}$ ,  $h_{G1} = 86.5 \text{ mm}$ ,  $h_{G2} = 84 \text{ mm}$ ,  $h_{G3} = 84.5 \text{ mm}$ ,  $d_{G1G2} = 2.69 \text{ mm}$ ,  $d_{G1G3} = 4.69 \text{ mm}$ , and  $d_{G2G3} = 3.28 \text{ mm}$ . The terminal grounded loads of the equivalent model are shown in Table IV.

Table II: Terminal grounded loads of the ten-conductor wiring harness.

	1	2	3	4	5	6	7	8	9	10
End 1	50 Ω	110 Ω	50 kΩ	2 Ω	2 kΩ	50 Ω	1 Ω	3 nH	2 pF	500 Ω
End 2	10 kΩ	5 Ω	200 Ω	400 Ω	10 Ω	50 Ω	1 pF	4pF	100 kΩ	10 nH

Table III: Terminal grounded loads of the nine-conductor wiring harness.

	1	2	3	4	5	6	7	8	9
End 1	50 Ω	50 Ω	10 Ω	100 Ω	15 Ω	1 MΩ	150 kΩ	1 kΩ	10 kΩ
End 2	10 Ω	1 MΩ	150 kΩ	15 kΩ	100 kΩ	10 Ω	15 Ω	15 Ω	100 Ω

$$[C]= \begin{bmatrix} 32.5 & -12.1 & -1.84 & -12.1 & -1.91 & -0.39 & -1.84 & -0.39 & -0.61 \\ & 39.2 & -12.1 & -2.19 & -9.03 & -2.19 & -0.39 & -0.18 & -0.39 \\ & & 32.5 & -0.39 & -1.91 & -12.1 & -0.61 & -0.39 & -1.84 \\ & & & 39.2 & -9.03 & -0.18 & -12.1 & -2.19 & -0.39 \\ & & & & 43.8 & -9.03 & -1.91 & -9.03 & -1.91 \\ & & & & & 39.2 & -0.39 & -2.19 & -12.1 \\ & & & & & & 32.5 & -12.1 & -1.84 \\ & & & & & & & 39.2 & -12.1 \\ & & & & & & & & 32.5 \end{bmatrix} \text{ pF/m} \quad (20)$$

$$[L]= \begin{bmatrix} 1170.4 & 890.9 & 749.9 & 893.2 & 821.6 & 727.6 & 754.6 & 729.9 & 680.6 \\ & 1165.8 & 886.2 & 821.6 & 888.5 & 816.9 & 729.9 & 749.9 & 725.3 \\ & & 1161.0 & 727.6 & 816.9 & 883.8 & 680.6 & 725.3 & 745.2 \\ & & & 1170.4 & 890.9 & 749.9 & 893.2 & 821.6 & 727.6 \\ & & & & 1165.8 & 886.2 & 821.6 & 888.5 & 816.9 \\ & & & & & 1161 & 727.6 & 816.9 & 883.9 \\ & & & & & & 1170.4 & 890.9 & 749.9 \\ & & & & & & & 1165.8 & 886.2 \\ & & & & & & & & 1161.0 \end{bmatrix} \text{ nH/m} \quad (21)$$

Table IV: Terminal grounded loads of the equivalent model.

	G1	G2	G3
End 1	50 Ω	5.1 Ω	856 Ω
End 2	10 Ω	11.8 kΩ	4.1 Ω

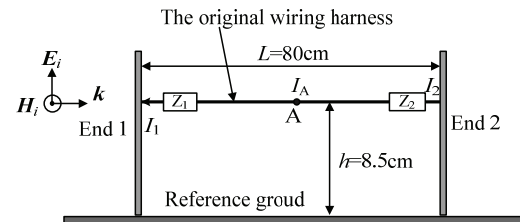
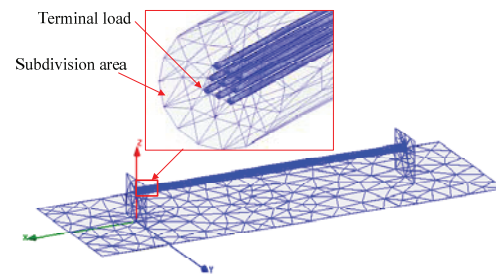


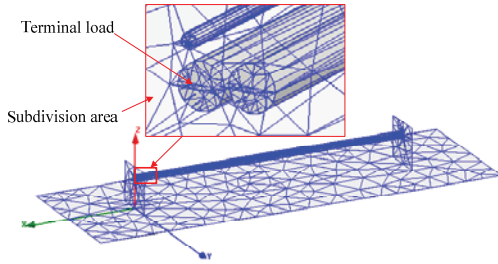
Fig. 9. EMR sensitivity model of the wiring harness.

**B. Simulation results and analysis**

The amplitude of the plane wave is 1 V/m, and the electric field is normal to the conductor. Figure 9 shows the nine-conductor wiring harness EMR sensitivity model. The EMR sensitivity model configuration of the equivalent group is the same as that in Fig. 9, except that the nine-conductor wiring harness is represented by three equivalent groups. Figure 10 (a) and (b) are the finite element mesh of the original wiring harness and the equivalent model, respectively. To improve the computation speed, subdivision principles are used.



(a) Finite element mesh of the nine-conductor wiring harness.



(b) Finite element mesh of the equivalent groups.

Fig. 10. Wiring harness finite element mesh.

Figures 11 to 13 show the common-mode current (sum of currents in all conductors) induced at End 1, End 2, and at the center point A of both models.

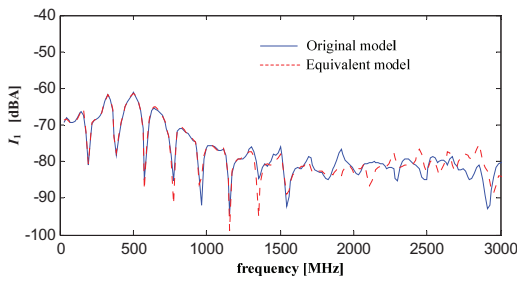


Fig. 11. Common-mode current induced at End 1.

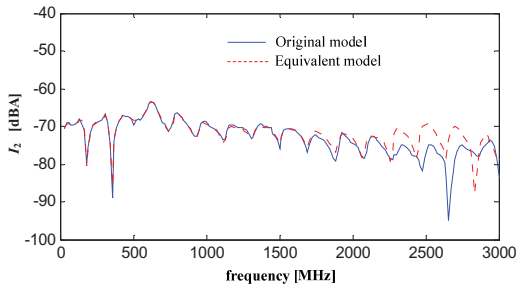


Fig. 12. Common-mode current induced at End 2.

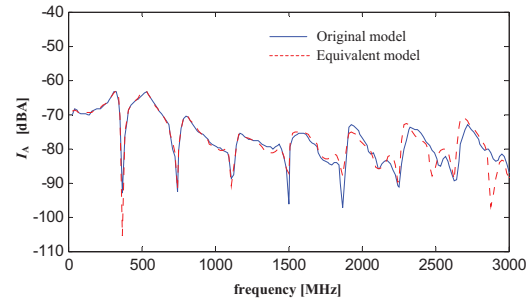


Fig. 13. Common-mode current induced at Point A.

The above three figures show that the common-mode currents induced in the original conductors and the equivalent model follow closely similar trends in the frequency range of 30 MHz to 3 GHz. Almost no discrepancy in amplitude was found from 30 MHz to 1.5 GHz. Meanwhile, the error increased from 1.5 GHz to 3 GHz. This finding indicates that several flaws could occur when circuit theory is used to solve the electromagnetic field problem at high frequency. Given that the automotive EMC standards are always in the frequency range of 30 MHz to 1 GHz, the equivalent model can be used as a simplified method in the EMR sensitivity problem in vehicle wiring harness.

**C. Comparison of the simulation resources**

In the case of the nine-conductor wiring harness, the simulation resources except for the modeling time are shown in Table V. The simulation was performed under the same conditions [e.g. frequency range (30 MHz to 3 GHz), discrete point numbers (201), calculation frequency and calculation region]. Table V shows that the mesh grid, calculation time, sweep time, computer memory, and disk space decreased. Thus, this method may be useful in modeling numerous automobile wiring harnesses.

Table V: Comparison of simulation resources.

	<b>Equivalent model</b>	<b>Original model</b>	<b>Ratio (%)</b>
Mesh grid quantity	22652	30515	74.23
Calculation time at center frequency	40 s	59 s	67.8
Sweep time	8485 s	12195 s	69.58
Memory	581 MB	796 MB	72.99
Disk space	958 MB	1198.08 MB	79.96

Table VI: Terminal load between conductors ( $\Omega$ ).

	Conductors in same groups			Conductors in different groups		
	G1	G2	G3	G1-G2	G1-G3	G2-G3
End 1	—	$Z_{23}=80$ $Z_{24}=200$ $Z_{35}=50$	$Z_{68}=80$ $Z_{78}=15$	$Z_{12}=50$ $Z_{14}=200$	$Z_{16}=80$	$Z_{26}=500$ $Z_{36}=20$
End 2	—	$Z_{45}=400$	$Z_{69}=5$ $Z_{78}=200$	$Z_{14}=36$ $Z_{15}=100$	$Z_{18}=50$	$Z_{47}=80$ $Z_{48}=400$ $Z_{56}=100$

**D. Validation of the equivalent method for the load between conductors**

Table VI shows the loads between conductors were added in the example in section III-B by using  $Z_{pq}$  representation. For the loads between conductors belonging to the same groups, the common-mode currents at End 2 are calculated as shown in Fig. 14. For the loads between conductors belonging to different groups, the currents at End 2 are obtained as indicated in Fig. 15.

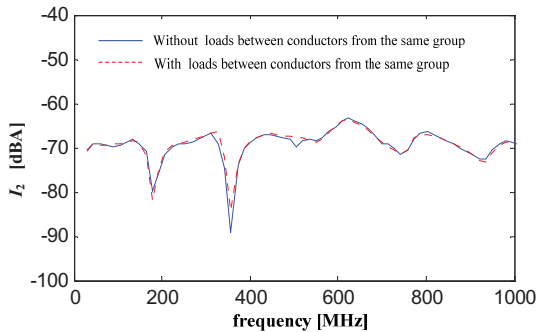


Fig. 14. Current at End 2 with and without the loads between conductors from the same group.

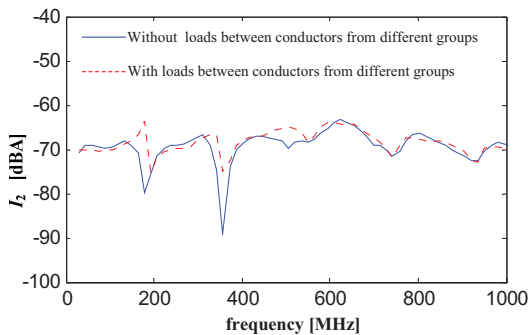


Fig. 15. Current at End 2 with and without the load between conductors from different groups.

Figure 14 illustrates that when conductors belong to the same group, the load between these conductors has no influence on the resonant frequency and amplitude of the current. Figure 15 shows that if the conductors belong to different groups, the load has no influence on the resonant frequency of the induced current, but can affect the amplitude with approximately 15 dB. Therefore, the load between conductors from the same group can be neglected, whereas the load between conductors from different groups needs equivalent processing.

Through the above handling method, the equivalent loads connected between equivalent groups ( $Z_{Gmn\_L}$ ) can be obtained, as shown in Table VII. Afterward, the current at End 2 can be calculated, as shown in Fig. 16.

Table VII: Terminal load between equivalent group conductors ( $\Omega$ ).

	Loads between equivalent groups		
	$Z_{G12\_L}$	$Z_{G13\_L}$	$Z_{G23\_L}$
End 1	40	80	19.2
End 2	26.5	50	40

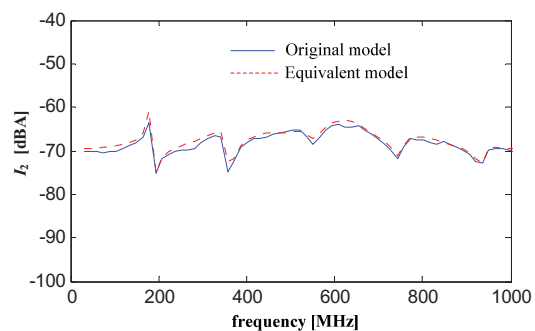


Fig. 16. Current at End 2 before and after the equivalent processing.

Figure 16 shows that after the equivalent processing, the currents were almost coincident with each other, indicating that the load equivalent method is functional.

### V. EXPERIMENTAL VALIDATION

#### A. Experimental arrangement

The experimental validation consisted of an 80 cm long seven-conductor wiring harness. The average height of the conductors is 18 mm above the reference ground. The distance between conductors is 2.6 cm. The radius of the conductors is 0.5 mm, surrounded by a 0.7 mm thick dielectric coating with a relative electric permittivity of 3.5 (neglected in the equivalent processing). Each end

of the wiring harness is supported by a metallic bracket measuring 12 cm high and 12 cm wide. Each end of the conductors is connected to the reference ground through the chip resistors, as shown in Table VIII.

The experimental test is carried out in a semi-anechoic chamber. Figure 17 shows the cross-section structure of the wiring harness and its arrangement. The transmitting antenna is a log-periodic antenna with a frequency range of 80 MHz to 3 GHz. The input power of the antenna is 13 dBm. A broadband current probe (F-65A from FCC Group International Inc., 10 kHz to 1 GHz) measures the common-mode current induced along the conductors. The test arrangement sketch map is described in Fig. 18.

Table VIII: Terminal grounded loads of the seven-conductor wiring harness ( $\Omega$ ).

	1	2	3	4	5	6	7
End 1	50 $\Omega$	50 $\Omega$	50 $\Omega$	50 $\Omega$	50 $\Omega$	50 $\Omega$	50 $\Omega$
End 2	50 $\Omega$	150 $\Omega$	20 $\Omega$	100 $\Omega$	150 k $\Omega$	300 k $\Omega$	100 k $\Omega$

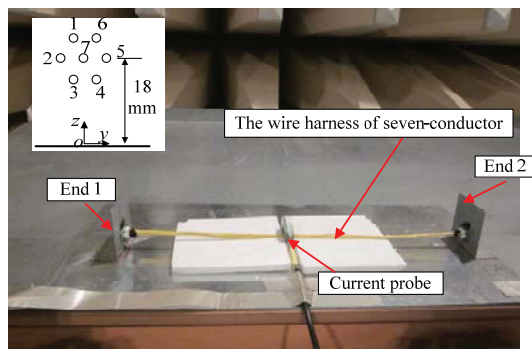


Fig. 17. Cross-section structure of the wiring harness and the wiring harness under test.

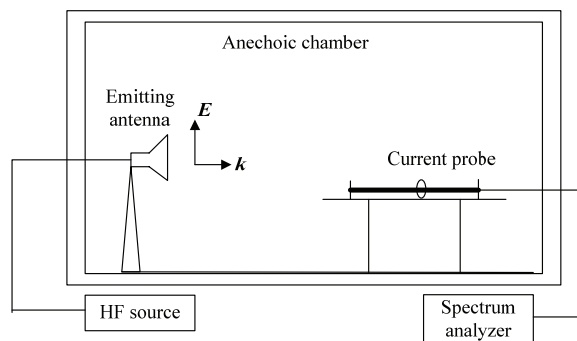


Fig. 18. Test arrangement sketch map.

#### B. Simulation model

Using the equivalent method, the wiring harness can be reduced to two equivalent groups. The simulation model is established in HFSS software, as shown in Fig. 19.

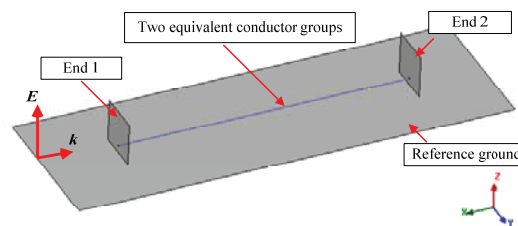


Fig. 19. Simulation model of EMR sensitivity in HFSS software.

#### C. Results and analysis

Figures 20 and 21 present the common-mode induced current measured on the conductors and the simulation results by FEM at End 2 and Point A (at the middle of the conductors), respectively. The two figures above show that the test results are consistent with the simulation results of both the original and the equivalent wiring harness. The results prove that the equivalent model is functional. Meanwhile, the test error increases with increasing frequency, and the error is 6 dB

approximately. Several reasons were identified to explain the degradation of the agreement. We assume that the effects of the parasitic parameters modify the termination loads. Moreover, the arrangement of the conductors is random, which changes the structure parameter, the p.u.l inductance and capacitance matrix. The log-periodic antenna modeling is another reason. However, we know there is an error in the EMC measurement and the error can be received within 6 dB.

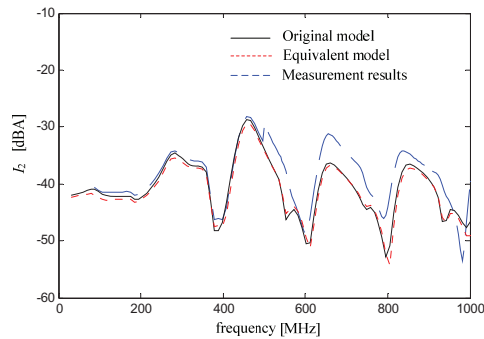


Fig. 20. Induced current at End 2.

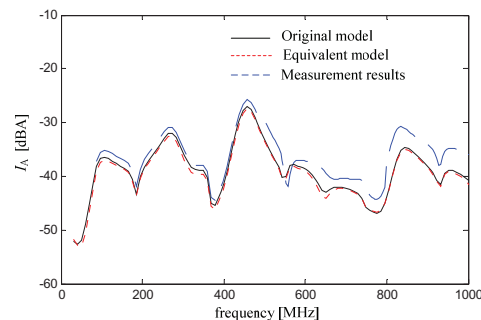


Fig. 21. Induced current at Point A.

## VI. CONCLUSIONS

This paper detailed the equivalent wave impedance concept and the induced current along the conductor generated by incident wave. The equivalent method was used for simulating the wiring harness induced current by FEM. The method aims to decrease the complexity of the wiring harness model and the computation time. After the numerical and experimental validation, the method was successfully applied to the wiring harness model physically adjacent to each other in high frequency.

This paper also outlined the wiring harness modeling process by FEM in HFSS. The vehicle model inhomogeneous medium can be easily dealt with in FEM, and thus method can be regarded as

a universal way to research EMC. With the whole automobile structure, wiring harness layout, major interference electromagnetic wave, the induced current along the conductors can be obtained through this efficient method.

## ACKNOWLEDGMENT

This work was supported by the Fundamental Research Funds for the Central Universities (No. CDJZR12110021).

## REFERENCES

- [1] C. Paul, *Introduction to Electromagnetic Compatibility (Second Edition)*, John Wiley & Sons, Inc., New York, 2006.
- [2] K. Yang, *Electromagnetic Compatibility Principles and Design Techniques*, Posts & Telecom Press, Beijing, 2004. (In Chinese)
- [3] X. Ma, *Research on the Pre-assessments of Electromagnetic Compatibility in Automobile*, Jilin University, 2008. (In Chinese)
- [4] C. Taylor, R. Satterwhite, and C. Harrison, "The response of a terminated two-wire transmission line excited by a nonuniform electromagnetic field," *IEEE Transactions on Antennas and Propagation*, vol. 13, no. 6, pp. 987-989, 1965.
- [5] A. Agrawal, H. Price, and S. Gurbaxani, "Transient response of multiconductor transmission lines excited by a nonuniform electromagnetic field," *IEEE Transactions on Electromagnetic*, vol. 22, no. 2, pp. 119-129, 1980.
- [6] F. Rachidi, "Formulation of field-to-transmission line coupling equations in terms of magnetic excitation field," *IEEE Transactions on Electromagnetic Compatibility*, vol. 35, no. 3, pp. 404-407, 1993.
- [7] J. Roden, "Coupled-pair transmission line termination revisited: an MTL approach," *Applied Computational Electromagnetics Society (ACES) Journal*, vol. 19, no. 2, pp. 18-23, July 2004.
- [8] M. Omid, Y. Kami, and M. Hayakawa, "Field coupling to nonuniform and uniform transmission lines," *IEEE Transactions on Electromagnetic Compatibility*, vol. 39, no. 3, pp. 210-211, 1997.
- [9] S. Tkatchenko, F. Rachidi, and M. Ianoz, "Electromagnetic field coupling to a line of finite length: theory and fast iterative solutions in the frequency and time domain," *IEEE Transactions on Electromagnetic Compatibility*, vol. 37, no. 4, pp. 509-518, 1995.
- [10] P. Papakanellos and G. Veropoulos, "Load response of terminate transmission lines exposed to external electromagnetic fields," *IET Microwaves, Antennas and Propagation*, vol. 4, no. 7, pp. 917-955, 2010.

[11] G. Antonini, G. Miscione, and J. Ekman, "PEEC modeling of automotive electromagnetic problems," *Applied Computational Electromagnetics Society (ACES) Journal*, vol. 23, no. 1, pp. 39-50, March 2008.

[12] S. Frei, R. Jobava, and D. Topchishvili, "Complex approaches for the calculation of EMC problems of large systems," *Electromagnetic Compatibility, 2004 IEEE International Symposium on*, California, no. 3, pp. 826-831, 2004.

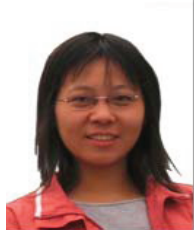
[13] L. Paletta, J. Parmantier, F. Issac, P. Dumas, and J. Alliot, "Susceptibility analysis of wiring in a complex system combining a 3-D solver and a transmission line network simulation," *IEEE Transactions on Electromagnetic Compatibility*, vol. 44, no. 2, pp. 309-317, 2002.

[14] G. Andrieu, L. Kone, F. Bocquet, B. Demoulin, and J. Parmantier, "Multiconductor reduction technique for modeling common-mode currents on cable bundles at high frequency for automotive applications," *IEEE Transactions on Electromagnetic Compatibility*, vol. 50, no. 1, pp. 175-184, 2008.

[15] B. Yang, X. Liu, and Y. Dai, *High Voltage Technology*, Chongqing: Chongqing University Press, 2001. (In Chinese)

[16] F. Tesche, V. Michel, and K. Torbjorn, *EMC Analysis Methods and Computational Models*, John Wiley & Sons, Inc., New York, 1997.

[17] Y. Peng, J. Ruan, Y. Zhang, and M. Li, "Calculation of very fast transient voltage distribution in pulse transformer," *Proceedings of the CSEE*, vol. 25, no. 11, pp. 140-145, 2005. (In Chinese)



**Yali Zheng** was born in Henan Province, China in 1982. She received her Ph.D. degree in Electrical Engineering from Chongqing University, Chongqing, China, in 2011. Her research interests include electromagnetic computation, electromagnetic compatibility and transmission-line analysis. Currently, she is a lecturer in the School of Electrical Engineering, Chongqing University.



**Quandi Wang** was born in Anhui province, China in 1954. She received her Ph.D. degree from the School of Electrical Engineering of Chongqing University, Chongqing, China, in 1998. Currently, she is a Professor in the School of Electrical Engineering, Chongqing University. Her main research interests are simulation

and numerical computation of electromagnetic field.



**Guohui Wang** was born in Gansu Province, China, in 1984. He received his M.C. degree in Electrical Engineering from Chongqing University, Chongqing, China, in 2009. Now, he works in Chengdu Qingbaijiang Power Supply Company of the State Grid. His current research interest is transmission-line analysis.



**Zongyu An** was born in Gansu Province, China, in 1986. He received his B.S. degree in Electrical Engineering from Chongqing University, Chongqing, China, in 2009. He is currently working toward the Ph.D. degree in the State Key Laboratory of Power Transmission Equipment & System Security and New Technology, Chongqing, China. His current research interest is vehicle electromagnetic compatibility.



**Qingsong Liu** was born in Sichuan Province, China, in 1975. He received his M.C. degree in Electrical Engineering from Chongqing University, Chongqing, China, in 2004. Then, he worked in Chongqing Vehicle Test & Research Institute. He is working toward his Ph.D. degree in the School of Electrical Engineering, Chongqing University Chongqing, China. His current research interest is vehicle electromagnetic compatibility.



**Xu Li** was born in Sichuan Province, China, in 1978. He received his Ph.D. degree in Electrical Engineering from Chongqing University, Chongqing, China, in 2008. He is currently a Senior Engineer in Automotive Engineering Institute of china chang'an Automobile Group. From July 2009 to May 2013 he is also working as a postdoctor in Institute of Electrical Engineering, Chinese Academy of Sciences. His main research interest is vehicle Electromagnetic Compatibility technology.